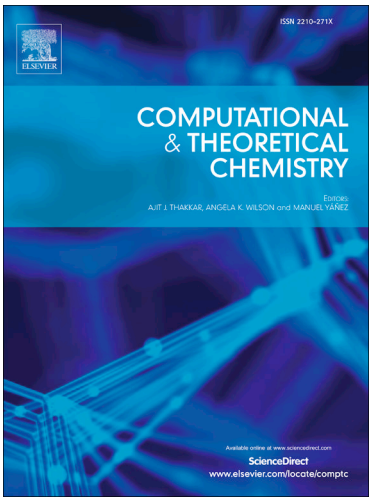


# Photophysical properties of chiral covalent organic cages

Qi Shi, Meng Sun, Jinmei Tian, Wenjie Zhang, Guochun Yang

PII: S2210-271X(17)30414-0
DOI: https://doi.org/10.1016/j.comptc.2017.09.016
Reference: COMPTC 2631

To appear in: *Computational & Theoretical Chemistry*

Received Date: 4 August 2017
Revised Date: 16 September 2017
Accepted Date: 20 September 2017

Please cite this article as: Q. Shi, M. Sun, J. Tian, W. Zhang, G. Yang, Photophysical properties of chiral covalent organic cages, *Computational & Theoretical Chemistry* (2017), doi: https://doi.org/10.1016/j.comptc.2017.09.016

# Photophysical properties of chiral covalent organic cages

Qi Shi, Meng Sun, Jinmei Tian, Wenjie Zhang and Guochun Yang*

*Centre for Advanced Optoelectronic Functional Materials Research and Laboratory for UV Light-Emitting Materials and Technology of Ministry of Education, National Demonstration Centre for Experimental Physics Education, Northeast Normal University, Changchun 130024, China.*

*E-mail:yanggc468@nenu.edu.cn*

Abstract: Chiral organic compounds are the excellent second-order nonlinear optical (NLO) materials due to their intrinsic non-symmetric structures and combined with the merits of organic compounds. Here, the ground electron structures, excited-state electron transition, and second-order NLO property of novel chiral covalent organic cages (COCs) [*J. Am. Chem. Soc. 2017, 139, 3348*], consisting of naphthalene-1,4:5,8-bis(dicarboximide) (NDI) units, have been fully investigated by DFT/TDDFT. The simulated electron absorption wavelengths are in good agreement with experimental ones, allowing us to assign their electron transition characters with high confidence. Based on the experimental structures, we designed eight compounds to probe the effect of different substitutions on photophysical properties. It is found that the substitution of $NH_2$ and $NO_2$ groups at opposite side of NDI and replacement of cyclohex-1,2-diyl with benzene are the most effective way to not only tune energy gaps and electron transition properties but also enhance the NLO response. For instance, the second-order NLO value of compound **2-h** is about 80 times as large as the organic urea molecule. Our work is also important for fully understanding photophysical properties and extending potential applications of chiral COCs.

**Keywords:** Chiral covalent organic cages; Electron transition; Nonlinear optical; DFT

## 1. Introduction

Nonlinear optics (NLO) has widespread applications (e.g. telecommunications, optical storage, and all-optical computing).[1-3] As a NLO material, large NLO response value is one of the necessary conditions for practical applications. Therefore, designing and synthesizing materials with large nonlinear optical (NLO) responses have attracted considerable attentions.[4-9] Among them, second-order NLO properties, deriving from the second-order polarization, are of the most immediate interest for practical applications. After continuous efforts and attempts, following two strategies have been proved to be greatly effective for enhancing the second-order NLO response. Specifically, one is the involvement of the electron donor and electron acceptor substitutions into the π-conjugated skeleton at appropriate positions.[10-14] In addition, second-order NLO response can be further enhanced by elevating electron-donor and electron-acceptor ability or extending the π-conjugation length.[15] The other way is the usage of chiral compounds, resulting from inherent non-symmetric structures.[16] Up to now, chiral compounds have been deemed as a valuable alternative in the search for new second-order NLO materials.[17-23] The role of chirality in second-order NLO has been reviewed.[24]

Much attention has been paid to the covalent organic cages (COCs) because of their rigid structures and broad applications (e.g. selective gas separation and organic electronics).[25-29] Very recently, a chiral COC, named as compound **3** consisting of three redox-active naphthalene-1,4:5,8-bis(dicarboximide) (NDI) units, was synthesized and well characterized (i.e. X-ray diffraction, $^{1}$H NMR, electron absorption spectra, circular dichroism spectra, and EPR spectrum).[30] NDI is the smallest homologue of rylene diimides, and exhibits perfectly planar, chemically robust, redox-active, electron-deficient.[31, 32] NDI and its derivatives have a variety of applications, ranging from biomedicine to electronics.[33, 34] It is noted that, in organic photovoltaic devices and flexible displays, NDI and its derivatives exhibit excellent thermal and oxidative stability, high electron affinity, high fluorescence quantum yield, and high carrier mobility.[31, 35-37] Studies have shown that the introduction of electron-withdrawing groups at the imide position of NDI usually causes a strong

π-electron polarization.[38] In compounds **3**, chiral cyclohex-1,2-diyl groups were involved into NDI and connected with aromatic imine. This special molecular architecture might offer some intriguing new opportunities for organic photoelectronic materials.

To fully understand the electron transition properties and find the potential applications, a number of compounds were studied, as show in Fig. 1. Among them, compound **1** is composed of a NDI fragment, two cyclohex-1,2-diyls and two aromatic imines, which can be considered as a basic structural unit of compounds **2** and **3**. Compound **2** is the dimerization compound **1**. The other compounds were designed to investigate the effect of donor or acceptor on second-order NLO and find the charge transfer cooperativity. In this work, with the help of density functional theory (DFT) calculations, our goal is to shed light on their frontier molecular orbitals distributions, electronic transition character, and the origin of second-order NLO.

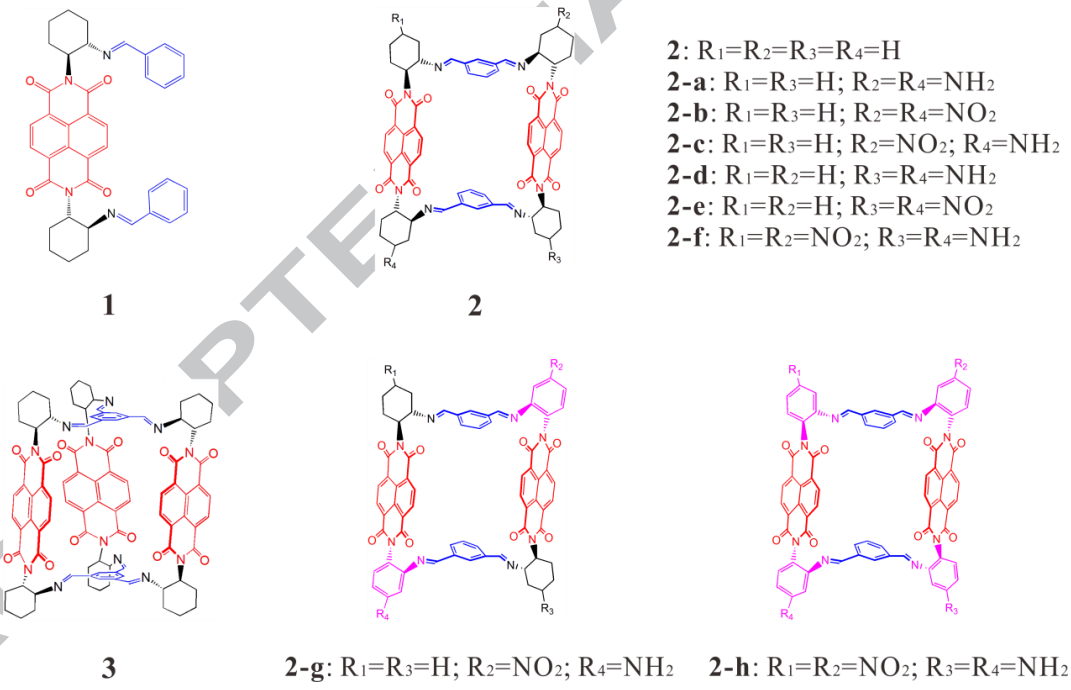


**Fig. 1** Chemical structures of the studied compounds. (NDI, red; cyclohex-1,2-diyl, black; aromatic imine, blue; benzene ring, purple.)

## 2. Computational details

All of the calculations were carried out in GAUSSIAN 09W program package.[39] The ground state geometries of the studied compounds (Fig. 1) have been fully optimized by using the B3LYP[40] functional, which is a combination of Becke's three-parameter hybrid exchange functional[40] and the Lee–Yang–Parr[41] correlation functional. During the process of optimization, there are no symmetry or internal coordination constraints. Basis sets of 6-31G(d) were applied. There are not any imaginary vibrational frequencies for all the optimized geometries, which confirmed that the optimized geometries were the local minima. The electron absorption energies and transition properties were studied at the TD-B3LYP/6-31G(d) level. We also probed the effect of different DFT functionals on the electron absorption wavelength.

Here, the hyper-Rayleigh scattering (HRS) was used to determine the second-order NLO properties, which can be described as:[42, 43]

$$\beta_{\mathrm{HRS}}=\sqrt{\langle\beta_{\mathrm{ZZZ}}^2\rangle+\langle\beta_{\mathrm{ZXX}}^2\rangle} \tag{1}$$

The associated depolarization ratio (DR), which gives the shape information of the NLO-phore, reads as follows:[44]

$$\mathrm{DR}=\frac{\langle\beta_{\mathrm{ZZZ}}^2\rangle}{\langle\beta_{\mathrm{ZXX}}^2\rangle} \tag{2}$$

$\beta$ is also typically decomposed into the sum of dipolar ($J$=1) and octupolar ($J$=3) tensorial components:[1]

$$\langle\beta_{\mathrm{ZZZ}}^2\rangle=\frac{9}{45}\left|\beta_{J=1}\right|^2+\frac{6}{105}\left|\beta_{J=3}\right|^2 \tag{3}$$

$$\langle\beta_{\mathrm{ZXX}}^2\rangle=\frac{1}{45}\left|\beta_{J=1}\right|^2+\frac{4}{105}\left|\beta_{J=3}\right|^2 \tag{4}$$

## 3. Results and discussion

### 3.1 Molecular structures and stability

The geometric structures of the studied compounds (Fig. 1) were fully optimized at the B3LYP/6-31G(d) level of theory. The absence of the imaginary frequency confirms that the optimized structures are the local minima. Compounds **1-3** have been synthesized and characterized by X-ray crystallography.[30] Compound **3** is taken as an example to test the reliability of our adopted functional and basis set. The optimized bond lengths along with experimental ones were shown in Table S1. It is found that the experimental bond lengths were well reproduced by our calculations except C–N bond. Specifically, our optimized C–N bond length is 0.053 Å larger than the experimental value. Similar phenomena were also observed in the compounds containing N atoms,[9, 45] which might be attributed to the limitation of the current method.

### 3.2 Electronic structures

It is well known that the electronic and optical properties are closely related to the HOMO/LUMO energy levels, the HOMO-LUMO gaps (energy gap), and the distributions of the frontier molecular orbitals (FMOs). Therefore, it is necessary to investigate these key parameters.

First, we investigated the effect of polymerization on energy levels or gaps of compounds **1-3**. Their HOMO/LUMO energy levels and energy gaps are nearly the same, as shown in Fig. 2. This indicates that the coupling between the NDI units are rather weak. To reduce the computational amount and keep the character of COCs, compounds **2** was taken as the basis to design the other compounds, named as **2a-2h**. Second, we discussed the single substitution at the different sides (i.e. $R_2$ and $R_4$ positions). Compared between **2** and **2-a**, the involvement of $NH_2$ on cyclohex-1,2-diyl groups at $R_2$ and $R_4$ positions mainly increases the HOMO energy level, whereas the LUMO energy level is almost unchanged (Fig. S1). Thus, the energy gap of compound **2-a** is smaller than that of compound **2**. For compound **2-b**, the incorporation of $NO_2$ equally decreases not only HOMO energy level but also LUMO energy level, leading that the energy gap of compound **2-b** is almost unchanged in comparison with compound **2**. As for compound **2-c**,

the substitution of $NO_2$ at $R_2$ and $NH_2$ at $R_4$ decreases the LUMO energy level, and increases the HOMO energy level, leading to the much smaller energy gap. This means that the simultaneous introduction of both $NH_2$ and $NO_2$ at opposite side can effectively adjust the energy gap. Third, compounds **2-d** and **2-e** contain double $NH_2$ or $NO_2$ substitutions at the same side of NDIs. Compound **2-f** involves double $NH_2$ and $NO_2$ substitutions at the different sides of NDIs. As we expected, their variations of the HOMO/LUMO energy levels are similar to those of compounds **2-a**-**2-c**. Compared with compound **2-c**, the energy gap of compound **2-f** is further reduced. Further compared between compounds **2-g** or **2-h** and **2-c** or **2-f**, the replacement of benzene for cyclohex-1,2-diyl significantly increases the HOMO energy level, while the LUMO energy level nearly unchanges. As a consequence, compounds **2-g** and **2-h** have the relatively smaller energy gaps. Generally, the smaller energy gap is, the higher second-order NLO response is, as will be discussed later.

The LUMOs of compounds **1-3** have a common character (i.e. primarily localize on the NDI fragments (Fig. 3). The same is true for the HOMOs, which are mainly distribute on the aromatic imines. Notably, the introduction of electron donor ($NH_2$) or electron acceptor ($NO_2$) groups breaks the symmetric distribution of the FMOs (Fig. 3 and S2). For example, the LUMO of compound **2-c** localizes on one NDI fragment, which is in sharp contrast with the LUMO on the two NDIs in compound **2**. Its HOMOs mainly on the substituted fragments. Based on the above discussion, both the HOMO/LUMO energy levels and the distribution of FMOs are tuned effectively, which would have a great impact on the photophysical properties.

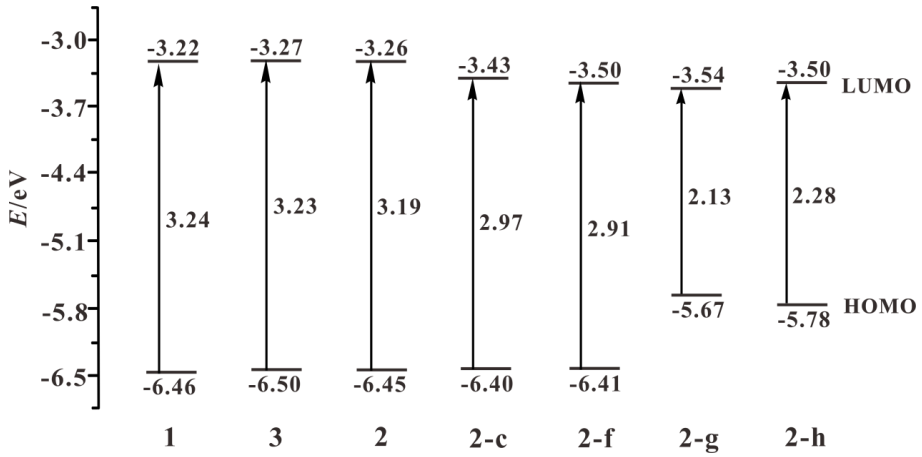


**Fig. 2** Schematic showing energy levels of compounds **1-3**, **2-c**, **2-f**, **2-g** and **2-h**.

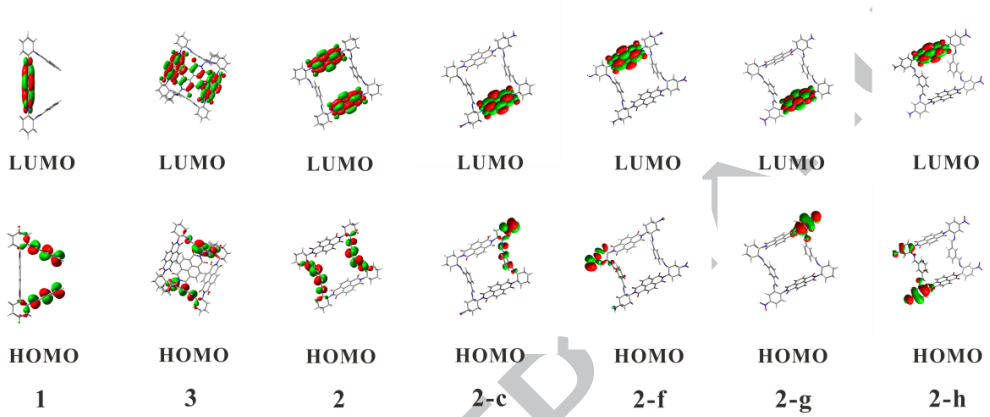


**Fig. 3** Frontier molecular orbital diagram of compounds **1-3**, **2-c**, **2-f**, **2-g** and **2-h**.

### 3.3 Electron transition

Time-dependent density functional theory (TDDFT) method has become one of powerful tools to study the electronic transition properties due to the balance between economy and accuracy.[46-49] To find suitable functionals for our studied compounds, four widely used DFT functionals (e.g. B3LYP,[40] CAM-B3LYP,[50-52] M05-2X,[53, 54] PBE1PBE[55, 56])were selected to calculate the electron absorption wavelengths of compound **1**, and compared with experimental values (Table S2). Among these considered functionals, the B3LYP perfectly reproduces the two experimental absorption wavelengths. Moreover, previous studies have shown that the B3LYP functional is the most suitable functional for organic compounds.[57-60] Thus, the absorption wavelengths, oscillator strengths, and major

contributions of the studied compounds were calculated at the B3LYP/6-31G(d) level, and summarized in Tables 1 and S3. It was found that the calculated absorption wavelengths of compounds **1-3** are in good agreement with the experimental ones (Table 1), indicating that our used method can reliably describe the electron transition properties. To assign their electron transition properties, the molecular orbitals (MO) involved into the main transition were shown in Fig. 4 and Fig. S3.

For all the studied compounds, only two electron absorption bands with the relatively large oscillator strengths were considered. For compounds **1-3**, the absorption wavelengths are nearly the same, whatever in shorter or longer wavelength region. These results again indicate the weak electron interaction between the NDIs. Moreover, the electron transition feature of these absorption bands are assigned as $\pi\rightarrow\pi^*$ character of NDI fragments (Fig. 4). With respect to the designed compounds **2-a**-**2-f**, the absorption wavelengths are close to compound **2**. However, the charge transfer (CT) characters have some differences compared with compound **2**. Besides the $\pi\rightarrow\pi^*$ of NDI, there are the charge transfer from substituents to NDI. These results mean that the introduction of donor ($NH_2$) or acceptor ($NO_2$) at different positions mainly affects the electron transition properties. Coming to the compounds **2-g** and **2-h**, the high-energy absorption wavelengths are obviously red-shifted compared with **2**, which is good agreement with the results of energy gaps. The high-energy band at 325.90 nm of compound **2-g** mainly results from HOMO-2→LUMO+3 and HOMO-4→LUMO+3 transitions, which can be assigned as $\pi\rightarrow\pi^*$ in aromatic imine part and nitrobenzene→aromatic imine CT. The low-energy absorption at 369.42 nm is described by HOMO-6→LUMO+1 and HOMO-17→ LUMO transitions with the $\pi\rightarrow\pi^*$ in NDI, aromatic imine→NDI, and nitrobenzene→NDI CT. The high-energy absorption of compound **2-h** at 340.91 nm is mainly described as $\pi\rightarrow\pi^*$ of aromatic imine, and benzene→aromatic imine CT. And the dominant electron transition of low-energy band (366.54 nm) is intramolecular CT between the two NDI units and minor aromatic imine→NDI CT. Overall, the introduction of donor ($NH_2$) or acceptor ($NO_2$) at different positions and enhancing conjugate degree (replacement of cyclohex-1,2-diyl with benzene) have

significant effects not only on the electron absorption wavelengths, but also on the electron transition properties.

**Table 1** Computed absorption wavelengths ($\lambda$ in nm) as compared to experimental data (in parentheses), oscillator strengths (*f*), and major contribution for compounds **1**-**3**, **2-g** and **2-h.**

| Compound | $\lambda$ | *f* | Major Contribution |
|---|---|---|---|
| **1** | 314.31(360.51) | 0.078 | H-12→L (85%) |
| | 369.85(382.94) | 0.330 | H-4→L (75%) |
| | | | H-2→L (21%) |
| **2** | 313.97(359.35) | 0.108 | H-20→L+1 (42%) |
| | | | H-21→L (41%) |
| | 368.24(382.24) | 0.675 | H-7→L (29%) |
| | | | H-6→L (27%) |
| **3** | 314.37(360.75) | 0.068 | H-29→L (20%) |
| | | | H-31→L+1 (19%) |
| | 367.16(381.31) | 0.929 | H-8→L (31%) |
| | | | H-9→L+1 (30%) |
| **2-g** | 325.90 | 0.095 | H-2→L+3 (73%) |
| | | | H-4→L+3 (13%) |
| | 369.42 | 0.287 | H-6→L+1 (22%) |
| | | | H-17→L (21%) |
| **2-h** | 340.91 | 0.162 | H-4→L+3(24%) |
| | | | H-5→L+2 (12%) |
| | 366.54 | 0.467 | H-7→L (31%) |
| | | | H-8→L+1 (17%) |

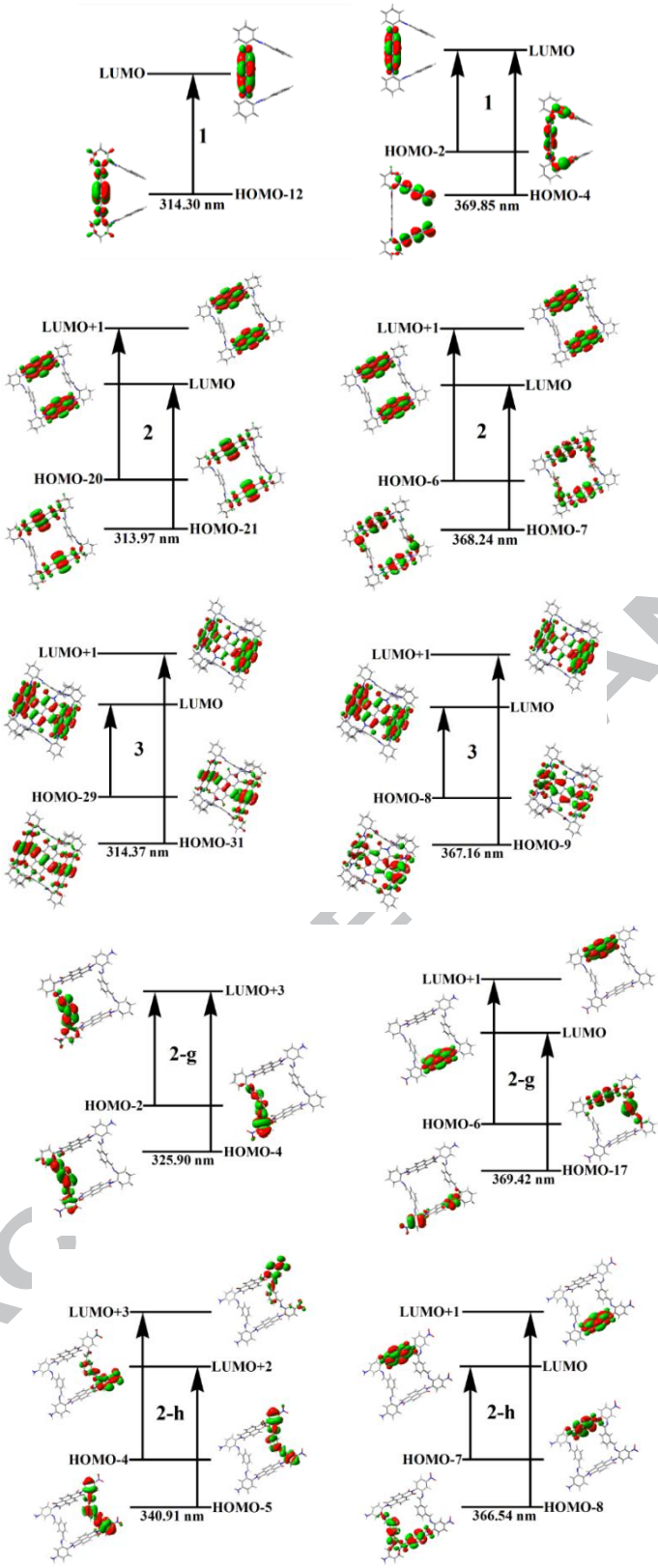


**Fig. 4** Molecular orbital isosurfaces involved in the main electron transitions of compounds **1-3**, **2-g** and **2-h** at the B3LYP/6-31G(d) level of theory.

### 3.4 Second-order NLO response

Chiral compounds have been viewed as a valuable alternative in the search for new second-order NLO materials due to their intrinsic non-centrosymmetric structures.[61] Based on above discussion, the studied compounds also exhibit obvious intramolecular charge transfer. Therefore, they might be the potential second-order NLO materials. Currently, DFT calculations have become a widely accepted method for predicting the novel NLO materials.[62, 63] Specifically, the B3LYP functional has been extensively used.[64-66] Thus, the calculated first hyperpolarizability ($\beta_{HRS}$) values of the studied compounds at the B3LYP/6-31G(d) level were given in Table 2.

The $\beta_{HRS}$ values of the studied compounds range from 0.179 to 14.011×$10^{-30}$ esu, indicating that subtle structural modifications can greatly enhance the second-order NLO response values. From compound **1** to **3**, the $\beta_{HRS}$ values decrease. It clearly indicates that the $\beta_{HRS}$ values is reverse to the number of repeat units. For the second-order NLO response, the higher asymmetry is, the larger $\beta_{HRS}$ is. The symmetry gradually increases from compound **1** to **3,** which can be confirmed by their dipole moments (1.250，0.732, 0.005 Debye).[30] On the other hand, the coupling between the NDI units are rather weak, as discussed before. For compounds **2-a**-**2-c**, the $\beta_{HRS}$ value of compound **2-a** is close to the compound **2**, which means that the introduction of $NH_2$ at opposite side ($R_2$, $R_4$ position) has little impact on the NLO properties. In contrast, the $\beta_{HRS}$ value of compound **2-b** is about 4.6 times as

large as compound **2.** It turned out that the introduction of the $NO_2$ substituted group is an effective strategy to increase the $\beta_{HRS}$ value. Astonishingly, the $\beta_{HRS}$ value of compound **2-c** is the largest among compounds **2-a**-**2-c.** As a result, asymmetric substitution of the $NH_2$ and $NO_2$ is an effective way to enhance the NLO response. Furthermore, the $\beta_{HRS}$ values of **2-d**-**2-f** are much larger than those of **2-a**-**2-c**. It demonstrates that the introduction two substitution groups on one side is more efficient than on opposite side. Similarly, electron acceptor ($NO_2$) is much conducive to raise the $\beta_{HRS}$ than donor ($NH_2$) group. Notably, the $\beta_{HRS}$ value of compound **2-f** becomes much larger, which proves again simultaneously introduce $NH_2$ and $NO_2$ groups is much practical. As expected, the $\beta_{HRS}$ values of compounds **2-g**-**2-h** are the largest, which is accordance with results of the energy gaps. So, substitution of $NH_2$ and $NO_2$ groups at opposite side of NDI and replacement of cyclohex-1,2-diyl with benzene is the most meaningful way to enhance the NLO response. The $\beta_{HRS}$ value of compound **2-h** is $14.011\times10^{-30}$ esu, which is about 83 times as large as the average second-order polarizability of the organic molecule urea.[14] Thus, our studied compounds are expected to become the potential second-order NLO materials. The depolarization ratio (DR) also is an important parameter for NLO materials, which can be used to unveil the contribution resulting from the part of the molecule.[1] Specifically, when the DR is smaller than 4.26, the octupolar component makes a major contribution.[1, 44, 67] Reversely, the $\beta_{HRS}$ response is dominantly from dipolar. For our studied compounds **1**-**3**, **2-a**, **2-b**, and **2-d**, the octupolar component is dominant. However, the dipolar part is larger than the octupolar for the designed

compounds **2-c**, **2-e**-**2-h**. This becomes more clearly from dipolar ($J$=1) and octupolar ($J$=3) tensorial components.

To explain their NLO origin, the electron density difference maps (EDDM) of compounds **2**, **2-g** were shown in Fig. 5. Obviously, the CT in NDIs is mainly responsible for the NLO origin of the compound **2**. However, the CT character in compound **2-g** is different from compound **2**. For instance, the EDDM located at 325.90 nm of compound **2-g** has the obvious nitrobenzene→aromatic imine CT. Therefore, the large NLO response originates from the large charge transfer character.

To provide more useful information for further experimental investigation, we calculated the frequency-dependent first hyperpolarizability by employing coupled perturbed Hartree–Fock theory. The frequency-dependent first hyperpolarizability values $\beta(-2\omega;\omega,\omega)$ for the second harmonic generation at 1907 and 1064 nm were shown in Table 2. Intriguingly, the frequency-dependent $\beta_{HRS}$ values become large as the frequency increases, especially for compounds **2-g** and **2-h**.

**Table 2** The calculated static first hyperpolarizability ($\beta_{HRS}$) values ($\times 10^{-30}$ esu), depolarization ratios (DRs), $|\beta_J|$ values ($\times 10^{-30}$ esu), and the frequency-dependent $\beta(-2\omega;\omega,\omega)$ values ($\times 10^{-30}$ esu) at specific frequencies (1907 and 1064nm) of the studied compounds at the B3LYP/6-31G(d) level of theory.

| Compound | $\beta_{HRS}$ | DR | $\lvert\beta_{J=1}\rvert$ | $\lvert\beta_{J=3}\rvert$ | $\beta_{HRS,1907}$ | $\beta_{HRS,1064}$ |
|---|---|---|---|---|---|---|
| **1** | 0.608 | 3.632 | 1.011 | 1.227 | 0.704 | 1.309 |
| **2** | 0.179 | 1.517 | 0.077 | 0.574 | 0.212 | 0.528 |
| **3** | 0.157 | 1.504 | 0.063 | 0.506 | 0.136 | 0.144 |
| **2-a** | 0.386 | 2.639 | 0.528 | 0.955 | 0.372 | 0.234 |

| | | | | | | |
|---|---|---|---|---|---|---|
| **2-b** | 0.828 | 1.949 | 0.839 | 2.385 | 0.963 | 1.444 |
| **2-c** | 2.232 | 6.136 | 4.406 | 2.645 | 2.567 | 3.941 |
| **2-d** | 0.830 | 3.869 | 1.419 | 1.595 | 0.893 | 1.124 |
| **2-e** | 2.368 | 5.150 | 4.468 | 3.505 | 2.757 | 4.482 |
| **2-f** | 3.036 | 5.355 | 5.792 | 4.302 | 3.484 | 5.638 |
| **2-g** | 8.070 | 5.216 | 15.345 | 11.733 | 9.218 | 24.592 |
| **2-h** | 14.011 | 5.003 | 26.336 | 21.304 | 16.260 | 35.383 |

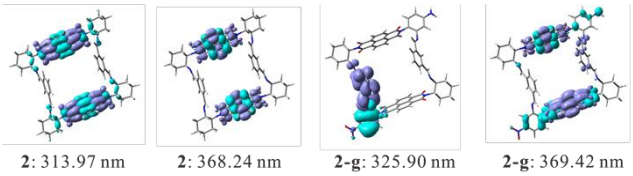


**Fig. 5** Electron density difference maps for compounds **2** and **2-g**. Blue and purple-colored areas indicate depletion and accumulation of electron density, respectively.

## 4. Conclusion

To understand photophysical properties and find the potential applications, we systemically investigated the geometric or electronic structures, electron absorption wavelength, and second-order NLO properties of eleven chiral COCs by using DFT/TDDFT. For the non-substituted COCs, their electron transition mainly originates from π→π* charge transfer of NDI fragments. Proper combination of $NH_2$ and $NO_2$ groups and extending conjugation can effective tune energy gaps, FMOs distributions, electron transition property, and NLO response. The charge transfer from π→π* of NDIs and nitrobenzene→aromatic imine is mainly responsible for the NLO response. In view of the second-order NLO value and intrinsic

non-centrosymmetric electronic structure, the studied chiral COCs have the possibility to be excellent second-order NLO materials.

## 5. Acknowledgements

This research was supported by Natural Science Foundation of China under No. 21573037, the Postdoctoral Science Foundation of China under grant 2013M541283, and the Natural Science Foundation of Jilin Province (20150101042JC).

## 6. Appendix A. Supplementary material

Supplementary data associated with this article can be found, in the online version, at http://dx.doi.org/10.1016/j.commatsci.2017.XXXX. (The compared bond-length between calculated and experimental measurement; the calculated excitation energies and oscillator strengths of compounds **2-a**-**2-f**; molecular orbitals)

## 7. Notes and references

[1] P. Beaujean, F. Bondu, A. Plaquet, J. Garcia-Amorós, J. Cusido, F.M. Raymo, F. Castet, V. Rodriguez, B. Champagne, Oxazines: A New Class of Second-Order Nonlinear Optical Switches, J. Am. Chem. Soc. 138 (2016) 5052-5062.
[2] N. Ma, L. Yan, W. Guan, Y. Qiu, Z. Su, Theoretical investigation on electronic structure and second-order nonlinear optical properties of novel hexamolybdate-organoimido-(car)borane hybrid, Phys. Chem. Chem. Phys. 14 (2012) 5605-5612.
[3] P. Singla, N. Van Steerteghem, N. Kaur, A.Z. Ashar, P. Kaur, K. Clays, K.S. Narayan, K. Singh, Multifunctional geometrical isomers of ferrocene-benzo[1,2-b:4,5-b[prime or minute]]difuran-2,6-(3H,7H)-dione adducts: second-order nonlinear optical behaviour and charge transport in thin film OFET devices, J. Mater. Chem. C 5 (2017) 697-708.
[4] B.J. Coe, Developing iron and ruthenium complexes for potential nonlinear optical applications, Coord. Chem. Rev. 257 (2013) 1438-1458.
[5] D. Escudero, W. Thiel, B. Champagne, Spectroscopic and second-order nonlinear optical properties of Ruthenium(ii) complexes: a DFT/MRCI and ADC(2) study, Phys. Chem. Chem. Phys. 17 (2015) 18908-18912.

[6] C. Wang, T. Zhang, W. Lin, Rational synthesis of noncentrosymmetric metal-organic frameworks for second-order nonlinear optics, Chem. Rev. 112 (2012) 1084-1104.
[7] H. Zhang, M. Zhang, S. Pan, X. Dong, Z. Yang, X. Hou, Z. Wang, K.B. Chang, K.R. Poeppelmeier, Pb17O8Cl18: A Promising IR Nonlinear Optical Material with Large Laser Damage Threshold Synthesized in an Open System, J. Am. Chem. Soc. 137 (2015) 8360-8363.
[8] Y. Si, G. Yang, Nonplanar donor-acceptor chiral molecules with large second-order optical nonlinearities: 1,1,4,4-tetracyanobuta-1,3-diene derivatives, J. Phys. Chem. A 118 (2014) 1094-1102.
[9] C. Liu, Y. Si, S. Shi, G. Yang, X. Pan, Understanding the photophysical properties of chiral dinuclear Re(i) complexes and the role of Re(i) in their complexes, Dalton Trans. 45 (2016) 7285-7293.
[10] J.Z. Liao, D.C. Chen, F. Li, Y. Chen, N.F. Zhuang, M.J. Lin, C.C. Huang, From achiral tetrazolate-based tectons to chiral coordination networks: Effects of substituents on the structures and NLO properties, Cryst. Eng. Comm. 15 (2013) 8180-8185.
[11] W. Wu, C. Li, G. Yu, Y. Liu, C. Ye, J. Qin, Z. Li, High-generation second-order nonlinear optical (NLO) Dendrimers that contain isolation chromophores: convenient synthesis by using click chemistry and their increased NLO effects, Chem. Eur. J. 18 (2012) 11019-11028.
[12] S.Y. Kim, M. Lee, B.H. Boo, Second molecular hyperpolarizability of 2,2′-diamino-7,7′-dinitro-9,9′- spirobifluorene: An experimental study on third-order nonlinear optical properties of a spiroconjugated dimer, J. Chem. Phys. 109 (1998) 2593-2595.
[13] T.C. Zeyrek, Theoretical Study of the N-(2,5-Methylphenyl)salicylaldimine Schiff Base Ligand: Atomic Charges, Molecular Electrostatic Potential, Nonlinear Optical (NLO) Effects and Thermodynamic Properties, J. Korean Chem. Soc. 57 (2013) 461-471.
[14] D.R. Kanis, M.A. Ratner, T.J. Marks, Design and construction of molecular assemblies with large second-order optical nonlinearities. Quantum chemical aspects, Chem. Rev. 94 (1994) 195-242.
[15] A. Plaquet, B. Champagne, J. Kulhánek, F. Bureš, E. Bogdan, F. Castet, L. Ducasse, V. Rodriguez, Effects of the Nature and Length of the π-Conjugated Bridge on the Second-Order Nonlinear Optical Responses of Push–Pull Molecules Including 4,5-Dicyanoimidazole and Their Protonated Forms, ChemPhysChem 12 (2011) 3245-3252.
[16] D. Cornelis, E. Franz, I. Asselberghs, K. Clays, T. Verbiest, G. Koeckelberghs, Interchromophoric interactions in chiral X-type pi-conjugated oligomers: a linear and nonlinear optical study, J. Am. Chem. Soc. 133 (2011) 1317-1327.
[17] Y. Liu, W. Xuan, Y. Cui, Engineering homochiral metal-organic frameworks for heterogeneous asymmetric catalysis and enantioselective separation, Adv. Mater. 22 (2010) 4112-4135.

[18] M. Gingras, One hundred years of helicene chemistry. Part 3: applications and properties of carbohelicenes, Chem. Soc. Rev. 42 (2013) 1051-1095.
[19] B.J. Coe, E.C. Harper, K. Clays, E. Franz, The synthesis of chiral, cationic nonlinear optical dyes based on the 1,1′-binaphthalenyl unit, Dyes pigm. 87 (2010) 22-29.
[20] Y. Si, G. Yang, Photophysical properties of azaboradibenzo[6]helicene derivatives, J. Mater. Chem. C 1 (2013) 2354.
[21] M. Kamiya, H. Sekino, T. Tsuneda, K. Hirao, Nonlinear optical property calculations by the long-range-corrected coupled-perturbed Kohn-Sham method, J. Chem. Phys. 122 (2005) 234111.
[22] J.M. Rivera, H. Reyes, A. Cortés, R. Santillan, P.G. Lacroix, C. Lepetit, K. Nakatani, N. Farfán, Second-Harmonic Generation within the P212121 Space Group, in a Series of Chiral (Salicylaldiminato)tin Schiff Base Complexes, Chem. Mater. 18 (2006) 1174-1183.
[23] J.D. Compain, P. Mialane, A. Dolbecq, J. Marrot, A. Proust, K. Nakatani, P. Yu, F. Secheresse, Second-order nonlinear optical properties of polyoxometalate salts of a chiral stilbazolium derivative, Inorg. Chem. 48 (2009) 6222-6228.
[24] A. Persoons, T. Verbiest, S. Van Elshocht, M. Kauranen, Application of Chiral Symmetries in Even-Order Nonlinear Optics, Chirality: Phys. Chem., American Chemical Society2002, pp. 145-156.
[25] T. Hasell, X. Wu, T.A. JonesJames, J. Bacsa, A. Steiner, T. Mitra, A. Trewin, D.J. Adams, A.I. Cooper, Triply interlocked covalent organic cages, Nat. Chem. 2 (2010) 750-755.
[26] Q. Song, S. Jiang, T. Hasell, M. Liu, S. Sun, A.K. Cheetham, E. Sivaniah, A.I. Cooper, Porous Organic Cage Thin Films and Molecular-Sieving Membranes, Adv. Mater. 28 (2016) 2629-2637.
[27] T. Tozawa, J.T.A. Jones, S.I. Swamy, S. Jiang, D.J. Adams, S. Shakespeare, R. Clowes, D. Bradshaw, T. Hasell, S.Y. Chong, C. Tang, S. Thompson, J. Parker, A. Trewin, J. Bacsa, A.M.Z. Slawin, A. Steiner, A.I. Cooper, Porous organic cages, Nat. Mater. 8 (2009) 973-978.
[28] D. Xu, R. Warmuth, Edge-Directed Dynamic Covalent Synthesis of a Chiral Nanocube, J. Am. Chem. Soc. 130 (2008) 7520-7521.
[29] G. Zhang, M. Mastalerz, Organic cage compounds--from shape-persistency to function, Chem. Soc. Rev. 43 (2014) 1934-1947.
[30] T. Solomek, N.E. Powers-Riggs, Y.L. Wu, R.M. Young, M.D. Krzyaniak, N.E. Horwitz, M.R. Wasielewski, Electron Hopping and Charge Separation within a Naphthalene-1,4:5,8-bis(dicarboximide) Chiral Covalent Organic Cage, J. Am. Chem. Soc. 139 (2017) 3348-3351.
[31] F. Wurthner, Perylene bisimide dyes as versatile building blocks for functional supramolecular architectures, Chem. Commun. (2004) 1564-1579.
[32] C. Huang, S. Barlow, S.R. Marder, Perylene-3,4,9,10-tetracarboxylic acid diimides: synthesis, physical properties, and use in organic electronics, J. Org. Chem. 76 (2011) 2386-2407.

[33] S. Guha, F.S. Goodson, L.J. Corson, S. Saha, Boundaries of anion/naphthalenediimide interactions: from anion-pi interactions to anion-induced charge-transfer and electron-transfer phenomena, J. Am. Chem. Soc. 134 (2012) 13679-13691.
[34] H.E. Katz, A.J. Lovinger, J. Johnson, C. Kloc, T. Siegrist, W. Li, Y.Y. Lin, A. Dodabalapur, A soluble and air-stable organic semiconductor with high electron mobility, Nature 404 (2000) 478-481.
[35] F. Wurthner, M. Stolte, Naphthalene and perylene diimides for organic transistors, Chem. Commun. 47 (2011) 5109-5115.
[36] X. Zhan, A. Facchetti, S. Barlow, T.J. Marks, M.A. Ratner, M.R. Wasielewski, S.R. Marder, Rylene and related diimides for organic electronics, Adv. Mater. 23 (2011) 268-284.
[37] B.A. Jones, A. Facchetti, M.R. Wasielewski, T.J. Marks, Tuning orbital energetics in arylene diimide semiconductors. Materials design for ambient stability of n-type charge transport, J. Am. Chem. Soc. 129 (2007) 15259-15278.
[38] M.A. Kobaisi, S.V. Bhosale, K. Latham, A.M. Raynor, S.V. Bhosale, Functional Naphthalene Diimides: Synthesis, Properties, and Applications, Chem. Rev. 116 (2016) 11685-11796.
[39] M.J. Frisch, G.W. Trucks, H.B. Schlegel, G.E. Scuseria, M.A. Robb, J.R. Cheeseman, G. Scalmani, V. Barone, B. Mennucci, G.A. Petersson, H. Nakatsuji, M. Caricato, X. Li, H.P. Hratchian, A.F. Izmaylov, J. Bloino, G. Zheng, J.L. Sonnenberg, M. Hada, M. Ehara, K. Toyota, R. Fukuda, J. Hasegawa, M. Ishida, T. Nakajima, Y. Honda, O. Kitao, H. Nakai, T. Vreven, J.A. Montgomery, Jr., J.E. Peralta, F. Ogliaro, M. Bearpark, J.J. Heyd, E. Brothers, K.N. Kudin, V.N. Staroverov, R. Kobayashi, J. Normand, K. Raghavachari, A. Rendell, J.C. Burant, S.S. Iyengar, J. Tomasi, M. Cossi, N. Rega, J.M. Millam, M. Klene, J.E. Knox, J.B. Cross, V. Bakken, C. Adamo, J. Jaramillo, R. Gomperts, R.E. Stratmann, O. Yazyev, A.J. Austin, R. Cammi, C. Pomelli, J.W. Ochterski, R.L. Martin, K. Morokuma, V.G. Zakrzewski, G.A. Voth, P. Salvador, J.J. Dannenberg, S. Dapprich, A.D. Daniels, Ö. Farkas, J.B. Foresman, J.V. Ortiz, J. Cioslowski, D.J. Fox, Gaussian, Inc., Wallingford CT, 2009.
[40] A.D. Becke, Density-functional thermochemistry. III. The role of exact exchange, J. Chem. Phys. 98 (1993) 5648-5652.
[41] C. Lee, W. Yang, R.G. Parr, Development of the Colle-Salvetti correlation-energy formula into a functional of the electron density, Phys. Rev. B 37 (1988) 785-789.
[42] A. Plaquet, M. Guillaume, B. Champagne, F. Castet, L. Ducasse, J.L. Pozzo, V. Rodriguez, In silico optimization of merocyanine-spiropyran compounds as second-order nonlinear optical molecular switches, Phys. Chem. Chem. Phys. 10 (2008) 6223-6232.
[43] F. Mançois, L. Sanguinet, J.L. Pozzo, M. Guillaume, B. Champagne, V. Rodriguez, F. Adamietz, L. Ducasse, F. Castet, Acido-triggered nonlinear optical switches: Benzazolo-oxazolidines, J. Phys. Chem. B 111 (2007) 9795-9802.
[44] M. de Wergifosse, J. de Ruyck, B. Champagne, How the Second-Order

Nonlinear Optical Response of the Collagen Triple Helix Appears: A Theoretical Investigation, J. Phys. Chem. C 118 (2014) 8595-8602.
[45] Y. Zhang, B. Champagne, Understanding the Second-Order Nonlinear Optical Properties of One-Dimensional Ruthenium(II) Ammine Complexes, J. Phys. Chem. C 117 (2013) 1833-1848.
[46] C.A. Guido, D. Jacquemin, C. Adamo, B. Mennucci, Electronic Excitations in Solution: The Interplay between State Specific Approaches and a Time-Dependent Density Functional Theory Description, J. Chem. Theory Comput. 11 (2015) 5782-5790.
[47] D. Jacquemin, B. Mennucci, C. Adamo, Excited-state calculations with TD-DFT: from benchmarks to simulations in complex environments, Phys. Chem. Chem. Phys. 13 (2011) 16987-16998.
[48] A. Wang, Y. Wang, J. Jia, L. Feng, C. Zhang, L. Liu, Theoretical analysis of the influence of chelate-ring size and vicinal effects on electronic circular dichroism spectra of cobalt(III) EDDA-type complexes, J. Phys. Chem. A 117 (2013) 5061-5072.
[49] D. Jacquemin, E.A. Perpète, G.E. Scuseria, I. Ciofini, C. Adamo, TD-DFT Performance for the Visible Absorption Spectra of Organic Dyes: Conventional versus Long-Range Hybrids, J. Chem. Theory Comput. 4 (2008) 123-135.
[50] A. Pedone, Role of Solvent on Charge Transfer in 7-Aminocoumarin Dyes: New Hints from TD-CAM-B3LYP and State Specific PCM Calculations, J. Chem. Theory Comput. 9 (2013) 4087-4096.
[51] T. Yanai, D.P. Tew, N.C. Handy, A new hybrid exchange–correlation functional using the Coulomb-attenuating method (CAM-B3LYP), Chem. Phys. Lett. 393 (2004) 51-57.
[52] K. Garrett, X. Sosa Vazquez, S.B. Egri, J. Wilmer, L.E. Johnson, B.H. Robinson, C.M. Isborn, Optimum Exchange for Calculation of Excitation Energies and Hyperpolarizabilities of Organic Electro-optic Chromophores, J. Chem. Theory Comput. 10 (2014) 3821-3831.
[53] Y. Zhao, N.E. Schultz, D.G. Truhlar, Design of Density Functionals by Combining the Method of Constraint Satisfaction with Parametrization for Thermochemistry, Thermochemical Kinetics, and Noncovalent Interactions, J. Chem. Theory Comput. 2 (2006) 364-382.
[54] Y. Zhao, N.E. Schultz, D.G. Truhlar, Exchange-correlation functional with broad accuracy for metallic and nonmetallic compounds, kinetics, and noncovalent interactions, J. Chem. Phys. 123 (2005) 161103.
[55] R. Orlando, V. Lacivita, R. Bast, K. Ruud, Calculation of the first static hyperpolarizability tensor of three-dimensional periodic compounds with a local basis set: A comparison of LDA, PBE, PBE0, B3LYP, and HF results, J. Chem. Phys. 132 (2010) 244106.
[56] C. Adamo, V. Barone, Toward reliable density functional methods without adjustable parameters: The PBE0 model, J. Chem. Phys. 110 (1999) 6158-6170.
[57] C. Liu, Y. Si, X. Pan, G. Yang, Photophysical properties of quinoxaline-fused

[7]carbohelicene derivatives, RSC Adv. 5 (2015) 72907-72915.
[58] Y.-L. Liu, J.-K. Feng, A.-M. Ren, Structural, electronic, and optical properties of phosphole-containing π-conjugated oligomers for light-emitting diodes, J. Comput. Chem. 28 (2007) 2500-2509.
[59] L. Yang, A.-M. Ren, J.-K. Feng, J.-F. Wang, Theoretical Investigation of Optical and Electronic Property Modulations of π-Conjugated Polymers Based on the Electron-Rich 3,6-Dimethoxy-fluorene Unit, J. Org. Chem. 70 (2005) 3009-3020.
[60] L.Y. Zou, A.M. Ren, J.K. Feng, Y.L. Liu, X.Q. Ran, C.C. Sun, Theoretical Study on Photophysical Properties of Multifunctional Electroluminescent Molecules with Different π-Conjugated Bridges, J. Phys. Chem. A 112 (2008) 12172-12178.
[61] E. Botek, J.-M. André, B. Champagne, T. Verbiest, A. Persoons, Mixed electric-magnetic second-order nonlinear optical response of helicenes, J. Chem. Phys. 122 (2005) 234713.
[62] M. Torrent-Sucarrat, J.M. Anglada, J.M. Luis, Evaluation of the Nonlinear Optical Properties for Annulenes with Hückel and Möbius Topologies, J. Chem. Theory Comput. 7 (2011) 3935-3943.
[63] Y. Zhang, B. Champagne, Theoretical Insight into the Second-Order NLO Response of the Bis{4-[2-(4-pyridyl)ethenyl]benzoato}-zinc(II) Metal–Organic Framework, J. Phys. Chem. C 116 (2012) 21973-21981.
[64] M.E. Defonsi Lestard, D.M. Gil, O. Estévez-Hernández, M.F. Erben, J. Duque, Structural, vibrational and electronic characterization of 1-benzyl-3-furoyl-1-phenylthiourea: an experimental and theoretical study, New J. Chem. 39 (2015) 7459-7471.
[65] E. Khan, A. Shukla, A. Srivastava, S. Shweta, P. Tandon, Molecular structure, spectral analysis and hydrogen bonding analysis of ampicillin trihydrate: a combined DFT and AIM approach, New J. Chem. 39 (2015) 9800-9812.
[66] P.K. Nandi, N. Panja, T.K. Ghanty, T. Kar, Theoretical Study of the Effect of Structural Modifications on the Hyperpolarizabilities of Indigo Derivatives, J. Phys. Chem. A 113 (2009) 2623-2631.
[67] K. Pielak, F. Bondu, L. Sanguinet, V. Rodriguez, B. Champagne, F. Castet, Second-Order Nonlinear Optical Properties of Multiaddressable Indolinooxazolidine Derivatives: Joint Computational and Hyper-Rayleigh Scattering Investigations, J. Phys. Chem. C 121 (2017) 1851-1860.

- Photophysical properties of chiral covalent organic cages were firstly studied.
- The electron transition properties of the studied compounds were assigned.
- The relation between substitutions and photophysical properties was established.
- Chiral covalent organic cages are the potential second-order NLO materials.